ORIGINAL ARTICLE

Journal of Cachexia, Sarcopenia and Muscle 2023; **14**: 493–507
Published online 5 January 2023 in Wiley Online Library (wileyonlinelibrary.com) **DOI:** 10.1002/jcsm.13153

Mitochondria transplant therapy improves regeneration and restoration of injured skeletal muscle

Stephen E. Alway[1,2,3,4]*, Hector G. Paez[1,2,3,5], Christopher R. Pitzer[1,2,3,5], Peter J. Ferrandi[2,5,6], Mohammad Moshahid Khan[2,7], Junaith S. Mohamed[2,4,6], James A. Carson[2,4,8] & Michael R. Deschenes[9]

[1]*Laboratory of Muscle Biology and Sarcopenia, Division of Regenerative and Rehabilitation Sciences, College of Health Professions, University of Tennessee Health Science Center, Memphis, TN, USA;* [2]*Center for Muscle, Metabolism and Neuropathology, Division of Regenerative and Rehabilitation Sciences, College of Health Professions, University of Tennessee Health Science Center, Memphis, TN, USA;* [3]*Department of Physiology, College of Medicine, University of Tennessee Health Science Center, Memphis, TN, USA;* [4]*Tennessee Institute of Regenerative Medicine, Memphis, TN, USA;* [5]*Integrated Biomedical Sciences Graduate Program, College of Graduate Health Sciences, University of Tennessee Health Science Center, Memphis, TN, USA;* [6]*Laboratory of Muscle and Nerve, Department of Diagnostic and Health Sciences, College of Health Professions, University of Tennessee Health Science Center, Memphis, TN, USA;* [7]*Department of Neurology, College of Medicine, University of Tennessee Health Science Center, Memphis, TN, USA;* [8]*Integrative Muscle Biology Laboratory, Division of Regenerative and Rehabilitation Sciences, College of Health Professions, University of Tennessee Health Science Center, Memphis, TN, USA;* [9]*Department of Kinesiology, College of William & Mary, Williamsburg, VA, USA*

Abstract

Background Injection of exogenous mitochondria has been shown to improve the ischaemia-damaged myocardium, but the effect of mitochondrial transplant therapy (MTT) to restore skeletal muscle mass and function has not been tested following neuromuscular injury. Therefore, we tested the hypothesis that MTT would improve the restoration of muscle function after injury.

Methods $BaCl_2$ was injected into the gastrocnemius muscle of one limb of 8–12-week-old C57BL/6 mice to induce damage without injury to the resident stem cells. The contralateral gastrocnemius muscle was injected with phosphate-buffered saline (PBS) and served as the non-injured intra-animal control. Mitochondria were isolated from donor mice. Donor mitochondria were suspended in PBS or PBS without mitochondria (sham treatment) and injected into the tail vein of $BaCl_2$ injured mice 24 h after the initial injury. Muscle repair was examined 7, 14 and 21 days after injury.

Results MTT did not increase systemic inflammation in mice. Muscle mass 7 days following injury was 21.9 ± 2.1% and 17.4 ± 1.9% lower ($P < 0.05$) in injured as compared with non-injured intra-animal control muscles in phosphate-buffered saline (PBS)- and MTT-treated animals, respectively. Maximal plantar flexor muscle force was significantly lower in injured as compared with uninjured muscles of PBS-treated (−43.4 ± 4.2%, $P < 0.05$) and MTT-treated mice (−47.7 ± 7.3%, $P < 0.05$), but the reduction in force was not different between the experimental groups. The percentage of collagen and other non-contractile tissue in histological muscle cross sections, was significantly greater in injured muscles of PBS-treated mice (33.2 ± 0.2%) compared with MTT-treated mice (26.5 ± 0.2%) 7 days after injury. Muscle wet weight and maximal muscle force from injured MTT-treated mice had recovered to control levels by 14 days after the injury. However, muscle mass and force had not improved in PBS-treated animals by 14 days after injury. The non-contractile composition of the gastrocnemius muscle tissue cross sections was not different between control, repaired PBS-treated and repaired MTT-treated mice 14 days after injury. By 21 days following injury, PBS-treated mice had fully restored gastrocnemius muscle mass of the injured muscle to that of the uninjured muscle, although maximal plantar flexion force was still 19.4 ± 3.7% ($P < 0.05$) lower in injured/repaired gastrocnemius as compared with uninjured intra-animal control muscles.

Conclusions Our results suggest that systemic mitochondria delivery can enhance the rate of muscle regeneration and restoration of muscle function following injury.

Keywords Mitochondria; Muscle injury; Regeneration; Muscle fibre types; Muscle force

Received: 22 May 2022; Revised: 17 November 2022; Accepted: 29 November 2022
**Correspondence to: Stephen E. Alway, The Tennessee Institute of Regenerative Medicine, 930 Madison Avenue, Suite 648, Memphis 38163, TN, USA.*
Email: salway@uthsc.edu

Introduction

Mitochondria function has both established and emerging roles in multiple muscle processes, including adenosine triphosphate (ATP) production,[1] apoptosis,[2] production of reactive oxygen species (ROS)[3] and control of muscle mass.[3] Traumatic muscle injury damages mitochondria,[4] which can cause leakage of their contents into the cytoplasm, triggering cell death,[2] elevating ROS,[5] increasing cytoplasmic calcium accumulation and causing endoplasmic reticulum stress. Furthermore, elevated ROS accumulation from damaged mitochondria[6,7] lowers mitochondrial 'quality' and induces a greater ratio of unhealthy to healthy mitochondria[8,9] that together reduce the available energy. These changes can suppress anabolic signalling and delay the restoration of neuromuscular structure and function after an injury.[10] While antioxidants may facilitate tissue repair,[5] this approach as a sole treatment for injury is only partially successful. For full restoration, there is a need to replace damaged mitochondria with healthy ones, which would correct the energy vacuum and potentially mitochondrial modulated signalling that is present with incomplete mitochondrial regeneration.

Mononucleated muscle stem cells/satellite cells (MSCs) are critical for muscle repair following an injury.[11,12] Previous observations indicate that the extracellular matrix, composed of muscle collagen/non-contractile tissue, may have an essential role in regulating MSC-induced muscle regeneration.[13,14] However, the importance of mitochondria available to MSCs or fibroblasts, to moderate MSC-directed muscle repair is unknown. Our previous work suggests that loss of SIRT1, an important regulator of mitochondrial biogenesis via activation of protein peroxisome proliferator-activated receptor-gamma coactivator 1α (PGC1α)[15] in MSCs, reduces the restoration of muscle function after an injury.[16] Further, reducing mitochondrial biogenesis and Drp1 expression increases fibrosis,[17,18] while reducing mitochondria-induced ROS accumulation can lower muscle fibrosis.[19] Because reducing PGC1α-regulated mitochondrial biogenesis can inhibit muscle repair, we hypothesized that increasing functional mitochondria in injured muscle would reduce muscle fibrosis and improve restoration of muscle function.

Multiple studies have shown that mitochondrial transplant therapy (MTT), which provides healthy donor mitochondria into ischaemic myocardium,[20–23] or skeletal muscle,[24] can improve recovery from ischaemia–reperfusion injury. Donor mitochondria can be incorporated into mesenchymal stem cells to improve arterial lung and cardiac tissue repair.[25,26] Nevertheless, it is unknown if MTT after traumatic muscle injury can improve the restoration of neuromuscular function. We hypothesized that systemic delivery of donor mitochondria would improve muscle mass and function while reducing fibrosis during recovery after injury. We report the novel finding that systemic mitochondria delivery can enhance muscle regeneration and restore muscle function following $BaCl_2$-induced injury.

Materials and methods

Animals and research design

All protocols were approved by the Institutional Animal Care and Use Committee of the University of Tennessee Health Science Center. Widespread muscle necrosis[27] was caused by injecting 50 μL of 1.2% $BaCl_2$ into the gastrocnemius muscle of one limb in male C57BL/6 mice (Jackson Labs, MA, USA) that were 8–12 weeks of age (n = 6–8). The right or left gastrocnemius was randomly injured with $BaCl_2$, and the opposite muscle was the non-injured (50 μL PBS-injected) control muscle.

Twenty-four hours after $BaCl_2$ injury, mice received a systemic injection of 50 μL PBS as a sham treatment, or 50 μg of isolated mitochondria diluted in 50 μL of PBS (MTT). In some experiments, donor mitochondria were stained with MitoTracker deep red. The muscles were collected 2 days after injury, to identify donor mitochondria, or markers of fibrosis. Serum and plasma were collected to assess for inflammatory markers 2 days after injury. $BaCl_2$-injured but sham-treated mice, received a tail injection of PBS. Gastrocnemius muscles from sham-treated mice were examined in control (C) or repairing (R) muscles after 7 days (7C,7R), 14 days (14C,14R) or 21 days of repair (21C,21R). Likewise control or repairing muscles in mice that received 50 μg of allogenic donor mitochondria were examined after 7 days (7CM,7RM), 14 days (14CM, 14RM) or 21 days of repair (21CM,21RM) following $BaCl_2$ injury. The research design of the study is shown in *Figure 1*.

Mitochondria isolation

Liver mitochondria were isolated from PhAM B6;129S-Gt (ROSA)26Sor$^{tm1.1(CAG-COX8A/Dendra2)Dcc}$/J or C57BL/6 mice (Jackson Labs) using the protocol modified from Preble et al.[22] Briefly, approximately 200 mg of liver was homogenized, filtered and centrifuged, and the mitochondria pellet was suspended in PBS for MTT, or mitochondrial respiration buffer, MiR05[28] for respirometric analysis.

Mitochondrial respiration

High-resolution respirometry was conducted on isolated mitochondria in MiR05[28] to ensure that isolated mitochondria

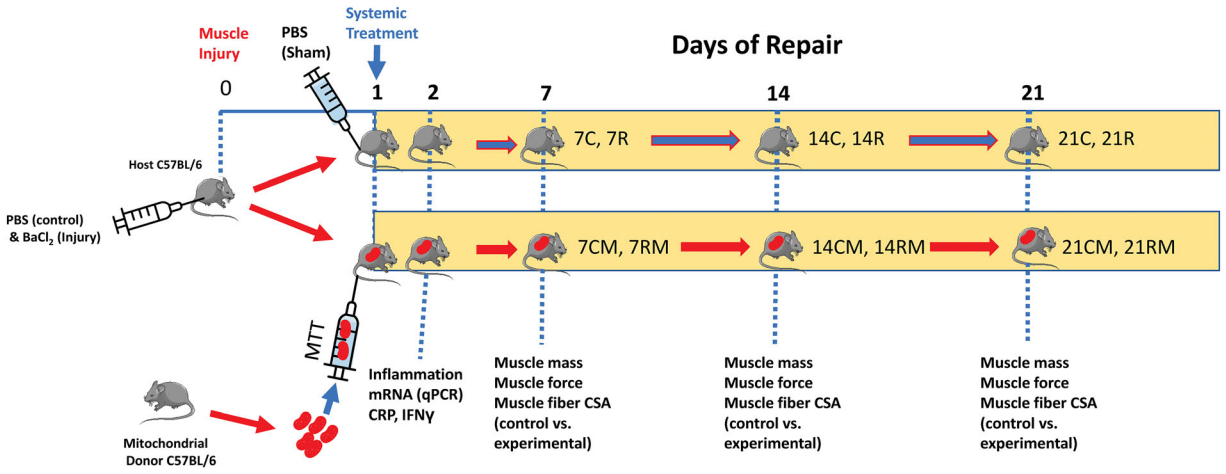

Figure 1 Research design. The study design is shown for the 21-day study. Mice received phosphate-buffered saline (PBS) injected into one gastrocnemius muscle, which acted as the non-injured intra-animal control. The contralateral gastrocnemius muscle was injected with $BaCl_2$ to cause muscle injury. Animals then received a systemic injection of PBS (sham treatment) or mitochondria (mitochondrial transplant therapy, MTT) treatment through a tail vein 24 h after $BaCl_2$ or PBS injection into the gastrocnemius muscles. In some acute experiments (2 days after muscle injury), mitochondria were stained with MitoTracker deep red prior to systemic injection, to identify if they were incorporated into the muscles of damaged mice. MTT was conducted on unstained mitochondria for experiments that were 7–21 days after muscle injury. Undamaged control muscles from PBS-sham treated animals were harvested 7 days (7C), 14 days (14C), or 21 days (21C), after BaCl2 injury to the contralateral gastrocnemius muscle. Injured-repairing gastrocnemius muscles from PBS-sham treated animals were also harvested after 7 days (7R), 14 days (14R) or 21 days (21R) following the $BaCl_2$ injury. Systemic delivery of 50 μg of mitochondria suspended in PBS was delivered via the tail vein in MTT-treated mice. Intra-animal control (PBS-injected, non-damaged) muscles of MTT-treated mice were designated as control, mitochondria treated (CM) muscles. The CM muscles were examined after 7 days (7CM), 14 days (14CM) or 21 days (21CM), after $BaCl_2$ or PBS injection. Repairing $BaCl_2$-injured muscles from MTT-treated animals (RM) were harvested after repair of 7 days (7RM), 14 days (14RM) or 21 days (21RM) following $BaCl_2$ injury. Outcome measures included muscle force, fatigue, muscle weight, fibre cross-sectional area and the percentage of collagen and other non-contractile tissue in injured-repaired and control non-injured muscles. Forty-eight hours after injury a subset of mice were examined for muscle inflammatory markers and plasma was collected for assessment of IFN-γ and C-reactive protein as markers for systemic inflammation.

were viable and respiration competent prior to transplantation (*Data S1*). This permitted assessment for State 2 LEAK respiration supported by complex I-linked substrates, and maximal State 3 oxidative phosphorylation through complex I.[29] The addition of 10 μM of Cytochrome *C* did not stimulate respiration >15%, indicating that the mitochondria were intact and respiration was competent. To confirm that mitochondria functioned normally after MTT, respiration was conducted on C2C12 cells 24 h after incubation with 50 μg/mL of isolated mitochondria or PBS (n = 4/group). Mitochondria respiration was normalized to the number of cells in the chamber[30] (*Data S2*).

Mitochondrial labelling and imaging

We used two *in vitro* and one *in vivo* approach to assess if donor mitochondria were incorporated into host muscle cells (*Data S3*). Donor mitochondria from PhAM mice have a Dendra-2 (GFP-green) label that permits their identification when they are incubated with C2C12 myoblasts or myotubes. Following 24 h of incubation in PhAM mitochondria, the cells were stained with MitoTracker deep red FM (ThermoFisher Scientific) to label all mitochondria.

In the third approach, 50 μg of MitoTracker-labelled mitochondria were injected in the tail vein of host C56BL/6 mice, and the mice were euthanized 24 h after MTT. Tissue cross sections or longitudinal sections were examined for MitoTracker-labelled mitochondria after incubation with an anti-dystrophin antibody to identify the muscle fibre sarcolemma (*Data S4*).

Muscle function

Plantar flexor force and fatigability were assessed in the injured limb or the intra-animal undamaged control limb 7, 14 or 21 days after injury to assess the role of MTT on muscle recovery following $BaCl_2$ injection. Function was measured with an 809C dynamometer (Aurora Scientific, Aurora, Canada). Plantar flexor muscles were activated by electric stimulation of the tibial nerve (200-μs pulse width) as previously described.[11,31,32] The left and right muscles were compared for each mouse, with one muscle having received

$BaCl_2$ (injured) and with the contralateral muscle receiving PBS (uninjured control muscle).

Fibre-type immunohistochemistry and cross-sectional area

The gastrocnemius muscles of both hind limbs were frozen and tissue sections were mounted on charged glass slides. The tissue sections were next incubated with primary antibodies (*Data S5*) to myosin heavy chain (MHC)-I, MHC IIA and MHC IIB as described previously.[11,16] The fluorescent images were developed with the appropriate secondary Alexa Fluor antibodies. Muscle fibre cross-sectional areas (CSAs) were obtained by planimetry from a minimum of 500 fluorescently labelled fibres/muscle taken from six to eight randomly selected fields at an objective magnification of ×20. Mean fibre area was calculated using ImageJ software (NIH, Bethesda, MD, USA).

Collagen and non-contractile proteins in regenerating muscles

To determine if MTT impacted the deposition of non-muscle tissue in regenerating muscle, we quantified the level of collagen non-muscle connective tissue from frozen tissue sections using *Gomori's Trichrome*. Stereological quantification of collagen and non-contractile tissue was obtained by point counting[33] using a 224-point grid in ImageJ software and expressed as percentage of the total tissue cross section.

qPCR analysis

RNA was isolated from control and injured muscles and reverse transcribed followed by real-time qPCR to amplify the transcripts (*Data S6*). The relative expression levels of gene transcripts transforming growth factor beta-1 (TGFβ1), type I collagen (COL I), type III collagen (COL III) and type V collagen (COL V) transcripts were estimated by the comparative CT method ($2^{-\Delta\Delta CT}$) and normalized to a housekeeping gene (GAPDH). We also measured transcriptional regulation of metalloproteinases (MMP)2, MMP9, MMP13 and MMP14.

Western immunoblot analysis of collagen and metalloproteinase proteins

To assess estimates of changes in proteins related to fibrosis of regenerating muscle, we conducted western blots for Collagen I, Collagen III, Collagen IV and MMP9 as these represented a subset of transcripts that suggested trends in changes after PBS as compared with MTT-treated muscles. The proteins were separated by SDS-polyacrylamide gels and transferred to nitrocellulose membranes then incubated with antibodies against Collagen I, III, IV and MMP9 (*Data S7*).

Systemic inflammation

To assess if systemic injection of autologous mitochondria resulted in a systemic inflammatory response, we assessed serum C-reactive protein (CRP) in uninjured mice that received no systemic treatment (n = 3), or after a systemic injection of PBS as a sham treatment (n = 3), or MTT (n = 4). A mouse CRP ELISA was conducted according to the manufacture's recommendations (*Data S8*).

As a further marker for systemic inflammation, comparisons were made between plasma levels of IFN-γ in control naive non-injured mice to determine if MTT resulted in a systemic inflammatory response (*Data S8*). Plasma IFN-γ was assessed in non-injured non-injected mice (n = 4), and in PBS-treated (n = 4), and MTT mice (n = 4), using by a mouse IFN-γ ELISA.

Statistical analysis

The statistical analysis was conducted with GraphPad-Prism 9 (GraphPad Software, San Diego, CA, USA) using a Two-way ANOVA (treatment × condition) with corrections made for multiple comparisons against a baseline control group by the Dunnett's test. Statistical differences between right and left hindlimbs of untreated or treated groups were compared using a One-way ANOVA. Gene changes were assessed from $2^{-\Delta\Delta CT}$ values using an unpaired T test on injured limbs; however, when, normality or equal variance were not met, a Mann–Whitney U test was conducted to assess differences in gene expression levels. The cumulative frequency of fibre size distributions was compared by Chi-squared analysis. The results were expressed as mean ± standard error of the mean (SEM), with significant differences established as $P < 0.05$.

Results

Mitochondrial incorporation

To assess if donor mitochondria are taken up by muscle cells, we isolated mitochondria from donor PhAM mice, which have a green Dendra-2 label, and incubated these mitochondria with C2C12 myoblasts and myotubes in culture. The Dendra-2 signal in the PhAM mitochondria remained green and did not change to red because the cells were excited with a light-emitting diode light source during imaging, and they were not exposed to a laser signal. Myoblasts were stained with MitoTracker Deep Red FM to identify their resident mitochondria. No Dendra-2 green mitochondria were found in control myoblasts that were not incubated with donor mito-

chondria (*Figure 2Ai*), but strong green labelling was seen around the nucleus of many C2C12 myoblasts (*Figure 2Aii*) and myotubes (*Figure 2Aiii*) 24 h after incubation with PhAM donor mitochondria. While some mitochondria appeared to be perinuclear, other transplanted mitochondria were taken up along the length of the myoblasts or myotubes. These findings were confirmed in experiments where C2C12 myoblasts were incubated with Dendra-2 donor mitochondria and then labelled with anti-Heat Shock Protein 60 (HSP-60, Invitrogen, USA), a mitochondria specific protein to label all mitochondria (donor + host mitochondria). These data show overlap of donor Dendra 2 mitochondria and the HSP60-labelled resident mitochondria (*Figure S1*). This indicated that donor mitochondria were incorporated into C2C12 cells.

To determine if mitochondria that are injected systemically would reach injured skeletal muscle, donor mitochondria from C57BL/6 mice were labelled with MitoTracker Deep Red then injected into the tail vein of mice 24 h after $BaCl_2$ injury of one limb. No donor mitochondria were found in the undamaged muscles 24 h after MTT (*Figure 2Bi*). However, we observed labelled mitochondria inside the muscle fibres that had been damaged by $BaCl_2$ (*Figure 2Bii,iii*) 24 h after MTT. MitoTracker-labelled mitochondria were found in longitudinal tissue sections where fibres that had a damaged sarcolemma, whereas mitochondria in non-damaged muscle fibres were rare (*Figure 2Biii*). These data show that mitochondria delivered systemically are taken up by damaged skeletal muscle. This is consistent with previously published data in damaged cardiac muscle.[20,21,23,34–36]

We found that mitochondria isolated from donor mice were fully functioning prior to MTT, with low Cytochrome *C* control efficiency (2.51% rise after 10-μM titration of Cytochrome *C*) (*Figure S2A*). Myoblasts incubated with isolated mitochondria show normal respiration (*Figure S2B*), indicating that mitochondrial integrity was maintained during isolation and after incorporation by the cells.

Skeletal muscle function

Representative maximal *in situ* muscle force records from undamaged control muscles (C) from PBS sham-treated mice and MTT-treated animals (CM) are shown in *Figure 3A*. Representative force records are also shown for repairing $BaCl_2$-injured-PBS sham treated animals (*Figure 3A*). Maximal muscle force was significantly lower in injured versus uninjured muscles of PBS- (−43.4 ± 4.2%, $P < 0.05$) and MTT-treated mice (−47.7 ± 7.3%, $P < 0.05$) 7 days after injury, but the reduction in force was not different between the experimental groups (*Figure 3B*). Muscle force was 38.5 ± 7% lower in muscles of 14C versus 14R mice and this did not differ from force in 7R mice. In contrast, MTT restored maximal muscle force by 14 days after injury (*Figure 3B*). Muscle force in PBS-treated mice had improved by 21 days after injury, but maximal force was still 19.4 ± 3.7% lower in 21R versus 21C mice. Furthermore, maximal force generated from 21RM mice was significantly greater than 21R mice (*Figure 3B*).

Muscle fatigue

As expected, gastrocnemius muscle fatigue was high (~88% loss of force) due to a high type IIB fibre population distribution in this muscle. In PBS-treated mice, muscle fatigue was lower in 7R (~58%) and 14R (61%) muscles, as compared with 7C and 14C muscles. Fatigue was lower in 7RM (65%) versus 7CM (88%), but fatigue was similar in 14CM and 14RM muscles. The fatigue response was not different between the 21R versus 21RM groups after injury (*Figure S3*).

Muscle mass is reduced with injury

Muscle mass was 21.9 ± 2.1% and 17.4 ± 1.9% lower ($P < 0.05$) in 7R and 7RM in muscles, respectively with no difference between the treatment conditions (*Figure 3C,D*). Muscle wet weight was significantly lower (−19.9 ± 2.3%) in 14R as compared with 14C muscles ($P < 0.05$). However, muscle weight was not different in 7R and 14R muscles of PBS-treated mice. Muscle weight was significantly greater in 14RM versus 14R muscles and the weight of 14RM muscles was only 3.9 ± 1.7% lower in 14RM versus 14CM ($P > 0.05$) (*Figure 3C,D*) in MTT-treated mice. The injured gastrocnemius muscle mass had recovered to that of uninjured muscles in 21R and 21RM mice (*Figure 3D*).

Fibre cross-sectional area

Type I and IIX fibres represented a very small percentage of the gastrocnemius muscle (*Figure S4*) and therefore were not analysed. Representative fibres from the control and injured gastrocnemius muscles from PBS-treated and MTT-treated mice are shown in *Figure 4A*.

Day 7 after injury

Mean Type IIA fibre CSA was 29.6 ± 3.6% lower (*Figure 4B*) and Feret diameter was 12.5 ± 2.9% lower (*Figure S5A*) in fibres from 7R versus 7C mice. Similarly, average Type IIA fibre CSA was 9.8 ± 3.6% lower (*Figure 4A*), and Feret diameter was 8.4 ± 2.6% lower (*Figure S5A*) in 7RM versus 7CM mice. The Type IIA fibre area-frequency distribution (*Figure 4C*) and the cumulative frequency data (*Figure 4E*) showed that approximately 93% of the Type IIA fibres had CSAs that were <1250 μm^2 7 days after injury 7R and 7RM muscles. Approximately 70% of the undamaged 7C fibres had areas that were <1250 μm^2 (*Figure 4C*). This was consistent with the shift to the left in the Type IIA Feret diameter

DOI: 10.1002/jcsm.13153

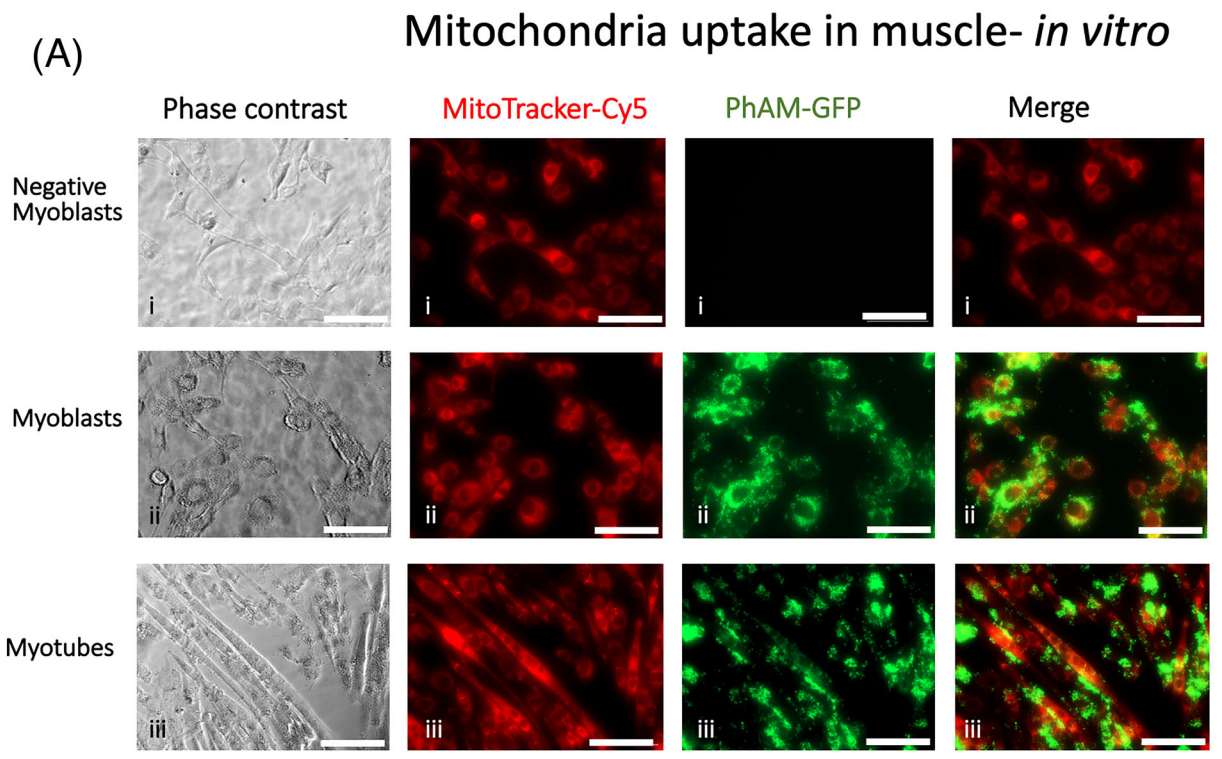
(A)
Mitochondria uptake in muscle- *in vitro*
Phase contrast
MitoTracker-Cy5
PhAM-GFP
Merge
Negative Myoblasts
Myoblasts
Myotubes
i
ii
iii

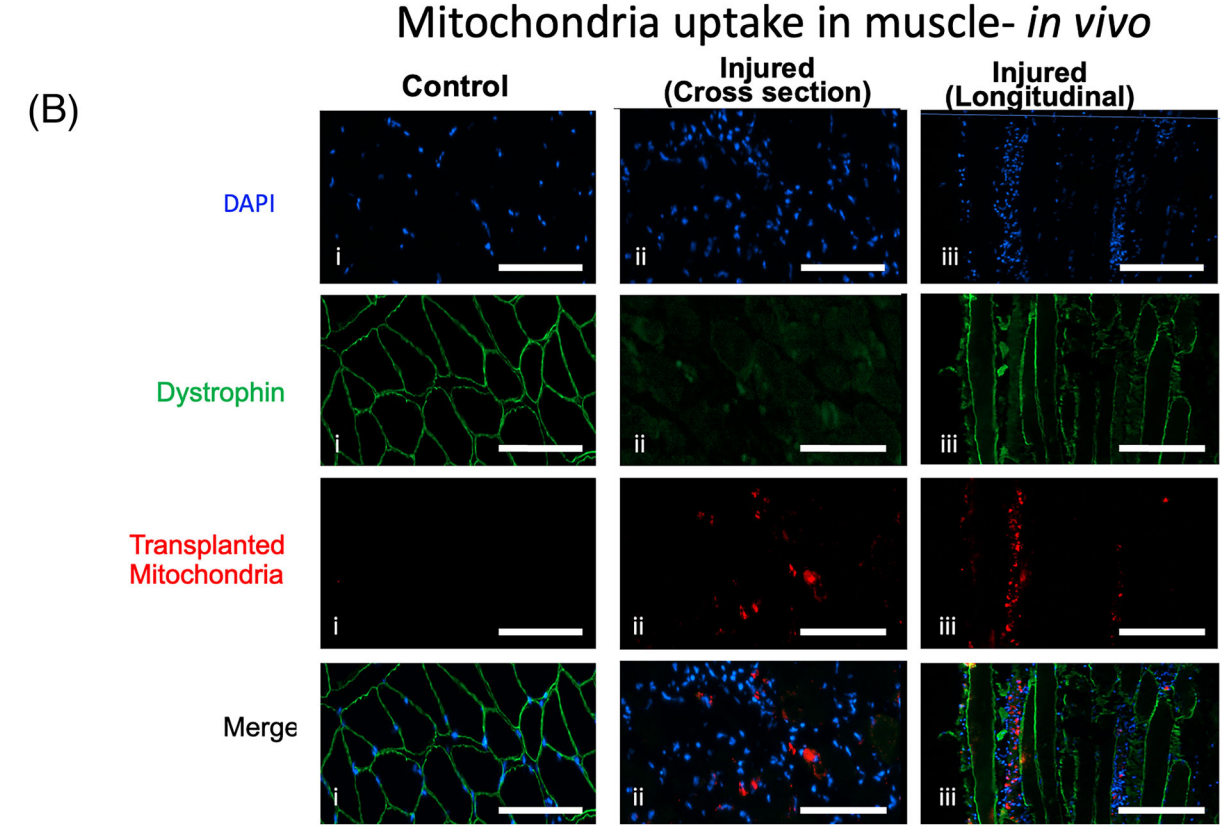
(B)
Mitochondria uptake in muscle- *in vivo*
Control
Injured (Cross section)
Injured (Longitudinal)
DAPI
Dystrophin
Transplanted Mitochondria
Merge
i
ii
iii

Figure 2 Uptake of donor mitochondria in myoblasts, myotubes and myofibres. (*A*) MitoTracker deep red was incubated on C2C12 cells to label resident mitochondria red (Cy5). Donor PhAM (green) mitochondria were isolated from Dendra-2 mice and incubated with MitoTracker-labelled C2C12 cells (i,ii) or myotubes (iii) at 37°C. C2C12 cells were grown to 70% confluency then differentiated into myotubes for 5 days using 2% horse serum (iii). Negative myoblasts (i) did not receive donor mitochondria. The cells were imaged 24 h later. Green donor mitochondria can be seen incorporated into the host C2C12 myoblasts and myotubes. Many donor mitochondria appear to be perinuclear. The scale bar corresponds to 200 μm. (*B*) Examples of mouse gastrocnemius tissue sections from mitochondrial transplant therapy (MTT) mice that were undamaged control muscles injected with phosphate-buffered saline (PBS) (i) or 2 days following injection with BaCl2 to induce muscle injury (ii,iii). Examples of injured muscles are shown in cross section (ii) or longitudinal section (iii). Mitochondria from C57BL/6 mice were isolated and labelled with MitoTracker deep red then injected into the tail vein of mice, 24 h after the $BaCl_2$ injury in one limb. Contralateral control (undamaged gastrocnemius muscles) in MTT mice (i) and BaCl2 injured muscle was cut at a thickness of 8 μm in cross section (ii) or longitudinal section (iii) and reacted with antibodies to dystrophin to identify the muscle sarcolemma and counter stained with DAPI to identify myonuclei. MitoTracker deep red stained the donor mitochondria red and where imaged in the Cy5 channel. The data show no red-stained mitochondria that were taken up by the contralateral control muscle (i), but some fibres that were damaged (as shown by disruption of the dystrophin in the fibre sarcolemma) took up the systemically delivered mitochondria. Longitudinal sections (iii) showed evidence of damaged fibres that has taken up labelled donor mitochondria. The scale bar corresponds to 200 μm.

distribution for repairing muscles of both 7R and 7RM mice (*Figure S5B*).

Mean Type IIB fibre CSA (*Figure 4B*) and Feret diameter (*Figure S5A*) were 63.3 ± 4.2% and 42.8 ± 4.4% smaller, respectively, in 7R, and 56.7 ± 4.4% and 48.1 ± 6.4% smaller, respectively in 7RM animals, as compared with 7C and 7CM, respectively. The Type IIB fibre-area frequency distribution (*Figure 4D*) and Type IIB fibre cumulative frequency data (*Figure 4E*) indicated that approximately 90% of the IIB fibres in the 7R and 7RM muscles were $<1750\ \mu m^2$, and this was compared with only approximately 15% of the population of Type IIB fibres in 7C muscles (*Figures 4D,F* and *S5C*).

Day 14 after injury

Representative tissue cross sections are shown for PBS sham-treated and MTT-treated mice 14 days after injury, in *Figure 5A*. Mean Type IIA fibre CSA (*Figure 5B*) and average Feret diameter (*Figure S5D*) was still 31.5 ± 1.5% less in 14R versus 14C muscle. However, fibre size was not significantly different between the 14R and 14RM mice. Similarly, there was no difference between Type IIA CSA or Feret diameter of 14C and 14CM. In contrast, the Type IIA fibre area distribution (*Figure 5C*) and the Type IIA cumulative frequency data (*Figure 5E*) showed that 87% and 81%, respectively, of the Type IIA fibres had CSA were $<1250\ \mu m^2$ 14 days in 14R and 14RM mice as compared with 75% and 88% of fibres in 7C or 7CM muscles, respectively, with fibres $<1250\ \mu m^2$ (*Figure S5D*).

Type IIB fibre CSA (*Figure 5B*) and Type IIB Feret diameter (*Figure S5D*) were 22.1 ± 2.8% and 24.6 ± 2.3% lower in 14R as compared with 14C mice. This compared with Type IIB CSA that was 3.9 ± 1.2% lower (*Figure 5B*) and Feret diameter that was 10 ± 2.1% (*Figure S5D*) lower in 14RM versus 14CM muscles. However, Type IIB fibre area had not recovered to control uninjured levels by 14 days after the $BaCl_2$ injury. The Type IIB fibre area frequency distribution (*Figure 5D*) and the cumulative frequency data (*Figure 5F*) showed that 78 ± 3.2% of the IIB fibres in 14R mice and 42 ± 2.4% of the IIB fibres in 14RM mice were significantly $<1750\ \mu m^2$, and this was compared with only 21 ± 1.8% of the Type IIB fibres in 14C mice and 26 ± 2.4% in 14CM muscles (*Figure S5D*). The Feret diameter distribution for Type IIB fibres (*Figure S5F*) showed the same pattern as the fibre area distribution.

Day 21 after injury

Representative tissue cross sections for control and repairing muscles 21 days post-injury are shown in *Figure 6A*. Type IIA fibres had similar mean fibre CSA (*Figure 6B*) and Feret diameters (*Figure S5G*) in 21C, 21CM, 21R and 21RM muscles. Average Type IIB fibre CSA (*Figure 6B*) and mean Feret diameter (*Figure S5G*) in 21R muscles had recovered to control levels. Type IIA fibre area-frequency (*Figure 6C*) and the cumulative frequency distribution (*Figure 6E*) was also similar in 14C, 14CM, 14R and 14RM groups. The Type IIA fibre Feret diameter frequency distribution was similar in 21C and 21R muscles, although the Type IIA Feret diameter frequency distribution had a greater percentage of fibres with diameters between 40–60 μm in the 21RM muscles as compared with 21C muscles (*Figure S5I*). Interestingly, the fibre area-frequency (*Figure 6D*) and the fibre cumulative frequency (*Figure 6F*) as well as the Type IIB fibre Feret data (*Figure S5I*) demonstrated the presence of a population of smaller Type IIB fibres in the PBS sham-treated muscles compared with the MTT-treated muscles. Specifically, 50.8 ± 4.3%, and 22.2 ± 2.2% of the Type IIB fibres in muscles of 21R and 21RM mice, respectively, were $<1750\ \mu m^2$. This compared with 16.1 ± 2.6% of the fibres in 21C and 27.7 ± 4.1% 21CM mice (*Figure S5I*).

Collagen and non-contractile muscle tissue

Gomori's trichrome staining (*Figure 7A*) showed that <9% of C and CM muscles contained collagen (non-contractile) tissue (*Figure 7B*). Picro Sirius red-stained collagen fibres showed a similar morphological distribution of non-contractile tissue (*Figure S6*). The percentage of non-contractile tissue was significantly greater in 7R (33.2 ± 0.2%) as compared with 7RM

DOI: 10.1002/jcsm.13153

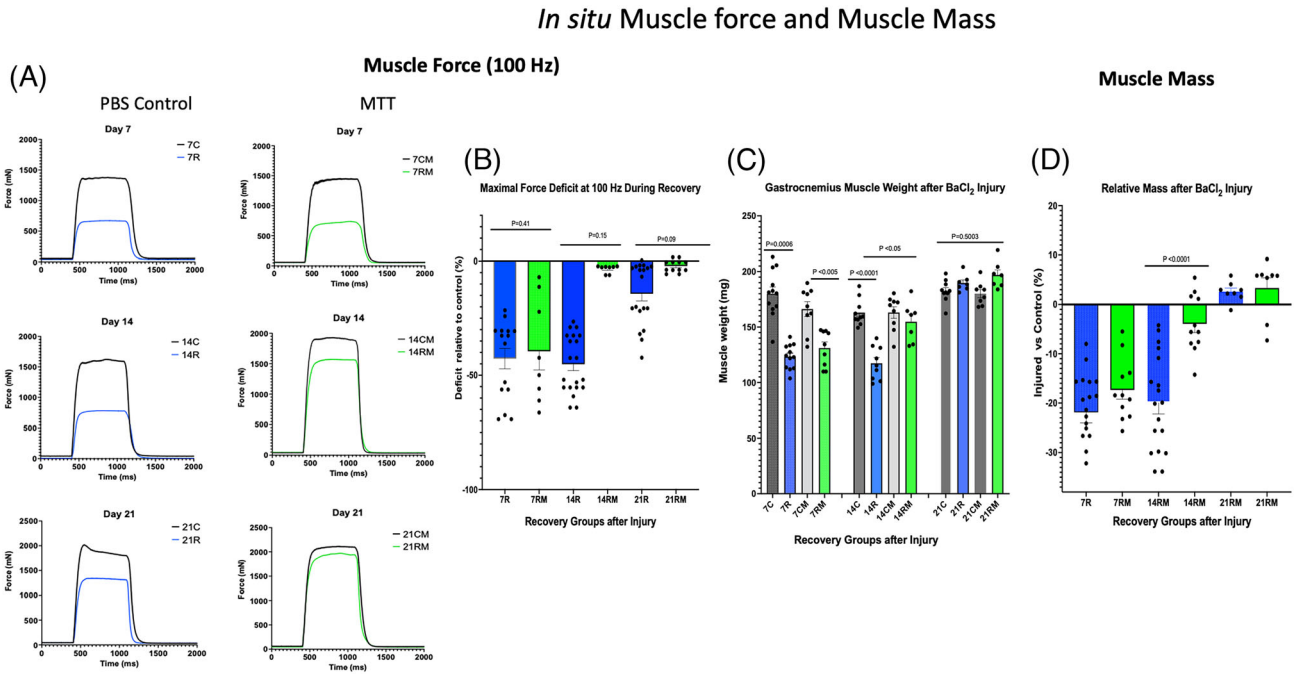

Figure 3 In situ muscle force and muscle mass. (*A*) Representative plantar flexor force records obtained at 100-Hz frequency for phosphate-buffered saline (PBS) sham-treated mice and mitochondrial transplant therapy (MTT)-treated mice 7, 14 or 21 days following $BaCl_2$ injury of the gastrocnemius on one leg. Control muscles (*C*) were injected with PBS and not injured. Control force records are for 7 days (7C), 14 days (14C) or 21 days (21C) after injury of the intra-animal control muscle. All $BaCl_2$-injured mice received a tail vein injection of PBS or MTT. PBS (sham-treated) mice were examined after 7 days of repair (7R), 14 days of repair (14R) or 21 days of repair (21R) following injury. Mice that received donor mitochondria (MTT-treated mice) were also examined after 7 days of mitochondria supplemented repair (7RM), 14 days of mitochondria repair (14RM) or 21 days of mitochondria repair (21RM) following injury. (*B*) the force deficit of the $BaCl_2$-injured muscle (expressed the percentage of the respective uninjured intra-animal control muscle) was measured 7 days post-injury in mice after systemic treatment with PBS (7R) or MTT (7RM). In other mice, the control and injured muscles were examined 14 days after injury in PBS-treated (14R) or MTT-treated (14RM), or after 21 days post-injury in PBS-treated (21R) or MTT-treated (21RM) gastrocnemius muscles. *P* values are shown over the data. (*C*) Absolute muscle wet weight was obtained in control and injured gastrocnemius muscles. Mice were injected systemically with PBS (sham) or with mitochondria (MTT). Control uninjured muscles from PBS-treated animals were obtained after 7 days (7C), 14 days (14C) or 21 days (21C) after injury of the opposite limb. Injured muscles of PBS-treated animals were examined or after 7 days of repair (7R), 14 days of repair (14R) or 21 days of repair (21R) following injury. Other injured mice received systemically delivered donor mitochondria (MTT treated). Control uninjured (PBS-injected) muscles from MTT-treated animals were obtained after 7 days (7CM), 14 days (14CM) or 21 days (21CM) after injury of the opposite limb. The damaged-repairing muscles were examined after 7 days of mitochondria-supplement repair (7RM), 14 days of mitochondria repair (14RM) or 21 days of mitochondria repair (21RM) following injury. *P* values are shown over the data. (*D*) The relative gastrocnemius muscle mass of the injured muscle is presented as a percentage of the corresponding uninjured (PBS-injected) intra-animal control muscle after 7 days after injury in PBS (7R) or MTT (7RM) mice, 14 days after injury in PBS (14R) or MTT (14RM) mice, or 21 days after injury in PBS (21R) or MTT (21RM) mice. There was a significant difference between PBS-treated and MTT-treated muscle for the 14-day group.

(26.5 ± 0.2%) muscles (*Figure 7B*). The percentage of non-contractile tissue was similar in gastrocnemius muscles 14R (15.9 ± 0.2%) and 14RM mice (11.1 ± 0.1%), but these were significantly less than 7R muscles (*Figure 7B*). The non-contractile composition of the gastrocnemius was not different between 21C, 21RM, 21R and 21RM muscles (*Figure 7B*).

Collagen gene expression

The relative gene expression of TGFβ1 mRNA was trending ($P = 0.08$) lower in muscles from 2RM versus 2R mice (*Figure 7C*). There was also a trend for lower gene expression of Collagen V ($P = 0.06$) and Collagen III ($P = 0.10$) in 2RM versus 2R muscles. However, Collagen I mRNA was not different between 2R and 2RM muscles.

Collagen protein abundance

Western blots (*Figure 7D*) showed a strong tendency ($P = 0.08$) for MTT-treatment to suppress Collagen IV protein abundance in 7RM versus 7R by 34%. However, Collagen I and III protein abundance was similar in 7RM and 7R muscles. (*Figure 7D*).

DOI: 10.1002/jcsm.13153

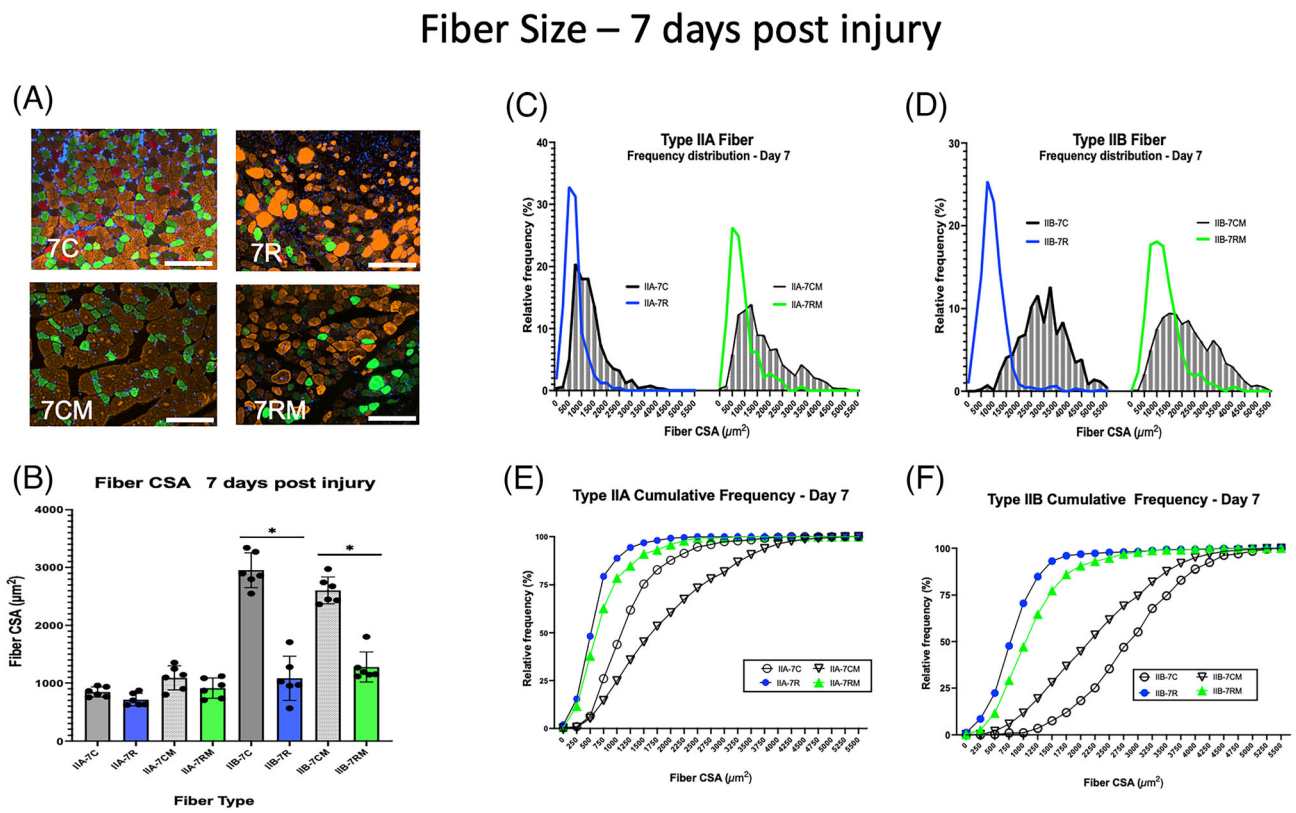

Figure 4 Muscle fibre size 7 days after $BaCl_2$ injury. (*A*) Examples of gastrocnemius cross sections of uninjured control muscles of phosphate-buffered saline (PBS)-injected mice (7C) or mitochondrial transplant therapy (MTT)-treated mice (7CM). Examples of muscle cross sections are shown that were injured and allowed to repair for 7 days after systemic PBS treatment (7R) and systemic MTT treatment (7RM). Fibre type was identified by immunocytochemistry of myosin heavy chains. Type IIA fibres (green), Type IIB fibres (orange/gold), Type IIX fibres (black) and Type I fibres (red). The white bar is 200 μm in length. (*B*) Mean fibre cross-sectional area (CSA) was obtained by planimetry from a minimum of 200 Type IIA and 200 Type IIB fibres in control non-injured muscles and 200 Type IIA and 200 Type IIB fibres in repairing muscles 7 days after the BaCl2 injury. The data are presented as mean ± *SD* for each animal. Control non-injured (PBS-injected) muscles from PBS-treated (7C) or MTT-treated mice (7CM). Injured ($BaCl_2$ injected) muscles from PBS sham-treated (7R) or MTT-treated mice (7RM). *Type IIB fibre CSA for 7C and 7CM were significantly greater than either 7R or 7RM Type IIB fibres at $P < 0.05$. (*C–F*) Fibre frequency histograms (C, D) and cumulative frequency distributions (E, F) for Type IIA (C, E) and Type IIB (D, F) fibres. (C, D) the corresponding control muscle data for the frequency histograms (7C or 7CM) are represented by shaded bars. The blue line represents data from PBS-injected mice 7 days post-injury (7R). The green line represents data from MTT-injected mice after 7 days of injury (7RM). (*E,F*) Cumulative frequency distribution for control muscle data (7C, circle or 7CM, inverted triangle). The blue line, PBS-injected mice 7 days post-injury (7R). The green line, MTT-injected mice after 7 days of injury (7RM).

Matrix metalloproteinases

mRNA levels of MMP13 in 2RM were lower than 2R muscles (*Figure 7E*). However, there was no difference in the relative transcript levels between 2R and 2RM for *MMP2*, *MMP9* and *MMP14* (*Figure 7E*). Furthermore, MMP9 protein abundance was similar in muscles from 7R-MMP9 and 7RM-MMP9 treated mice (*Figure 7D*).

Systemic inflammation

There was no difference in plasma levels of IFN-γ (*Figure 7F*) between PBS-treated and MTT-treated mice 2 days after $BaCl_2$ injury. Similarly, serum CRP levels were not different, 2 days after systemic delivery of PBS or MTT. Furthermore, PBS- and MTT-treated mice CRP levels did not differ from control mice that did not receive either treatment (*Figure 7G*). Thus, the data do not show any evidence of MTT-induced systemic inflammation.

Discussion

$BaCl_2$ causes myofibre Ca^{2+} overload and hyper-contractions, leading to widespread muscle proteolysis and membrane rupture.[37] Motor innervation is also disrupted but MSCs are unharmed.[27] We report that systemic delivery of healthy donor mitochondria to mice with a $BaCl_2$ injured muscle improved muscle repair and restoration of function.

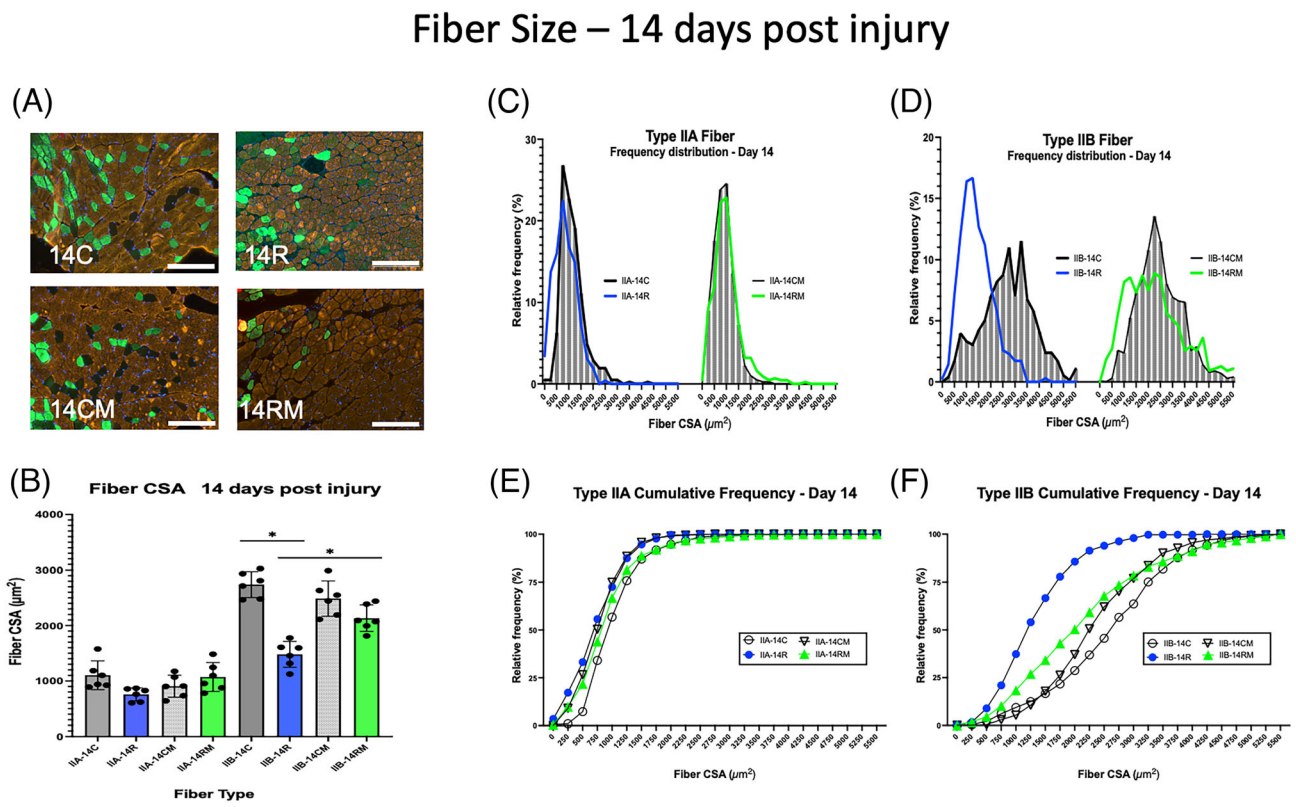

Figure 5 Muscle fibre size 14 days after $BaCl_2$ injury. (*A*) Examples of gastrocnemius cross sections of uninjured control muscles of phosphate-buffered saline (PBS)-injected mice (14C) or mitochondrial transplant therapy (MTT)-treated mice (14CM). Examples of muscle cross sections are shown, where injured muscles were allowed to repair for 14 days after systemic PBS sham- treatment (14R) and systemic MTT-treatment (14RM). Fibre type was identified by immunocytochemistry of myosin heavy chains. Type IIA fibres (green), Type IIB fibres (orange/gold), Type IIX fibres (black) and Type I fibres (red). The white bar is 200 μm in length. (*B*) Mean fibre cross-sectional area (CSA) was obtained by planimetry from a minimum of 200 Type IIA and 200 Type IIB fibres in control non-injured muscles and 200 Type IIA and 200 Type IIB fibres in repairing muscles 14 days after the BaCl2 injury. The data are presented as mean ± *SD* for each animal. Control non-injured (PBS-injected) muscles from PBS-treated (14C) or MTT-treated mice (14CM). Injured ($BaCl_2$ injected) muscles from PBS sham-treated (14R) or MTT-treated mice (14RM). *Type IIB fibre CSA for 14C was significantly greater than either 14R or 14RM Type IIB fibres at $P < 0.05$. Type IIB fibre CSA for 14C and 14RM was significantly greater than 14R at $P < 0.05$. (*C–F*) Fibre frequency histograms (*C,D*) and cumulative frequency distributions (*E,F*) for Type IIA (*C,E*) and Type IIB (*D,F*) fibres. (*C,D*) The corresponding control muscle data for the frequency histograms (14C or 14CM) are represented by shaded bars. The blue line represents data from PBS-injected mice 14 days post-injury (14R). The green line represents data from MTT-injected mice after 14 days of injury (14RM). (*E,F*) Cumulative frequency distribution for control muscle data (14C, circle or 14CM, inverted triangle). The blue line represents PBS-injected mice 14 days post-injury (14R). The green line represents MTT-injected mice after 14 days of injury (14RM).

Transplanted mitochondria appeared healthy

Previous studies have shown that MTT provides healthy donor mitochondria, which enhances repair of ischaemic myocardium,[20–23] or skeletal muscle[24] and also improves outcomes from neurological diseases.[38] MTT-treated myoblasts respired similarly to non-MTT-treated myoblasts (*Figure S2*). It was not unexpected that the maximal respiration did not increase in MTT-treated myoblasts. However, we cannot rule out the possibility that there was a transient increase in respiration and our sampling point missed this increase. Such a transient increase in respiration has been shown in MTT-treated cardiomyocytes,[39] and then respiration returned to that of control cardiomyocytes. Alternatively, it is possible is that the rapid proliferation of myoblasts may 'dilute' the respiratory enhancement by MTT, as these cells will easily double by 24 h, and the daughter cells will not be as loaded with exogenous donor mitochondria. Furthermore, post-mitotic cells or cells undergoing stress (from injury) may be better equipped to keep the spare respiratory capacity as they rely heavily on oxidative phosphorylation for energy during muscle repair.

Restoration of muscle structure and function after injury

As expected, $BaCl_2$ injected into the gastrocnemius resulted in muscle necrosis and a loss of muscle weight, which then began a process of muscle regeneration, but muscle weight

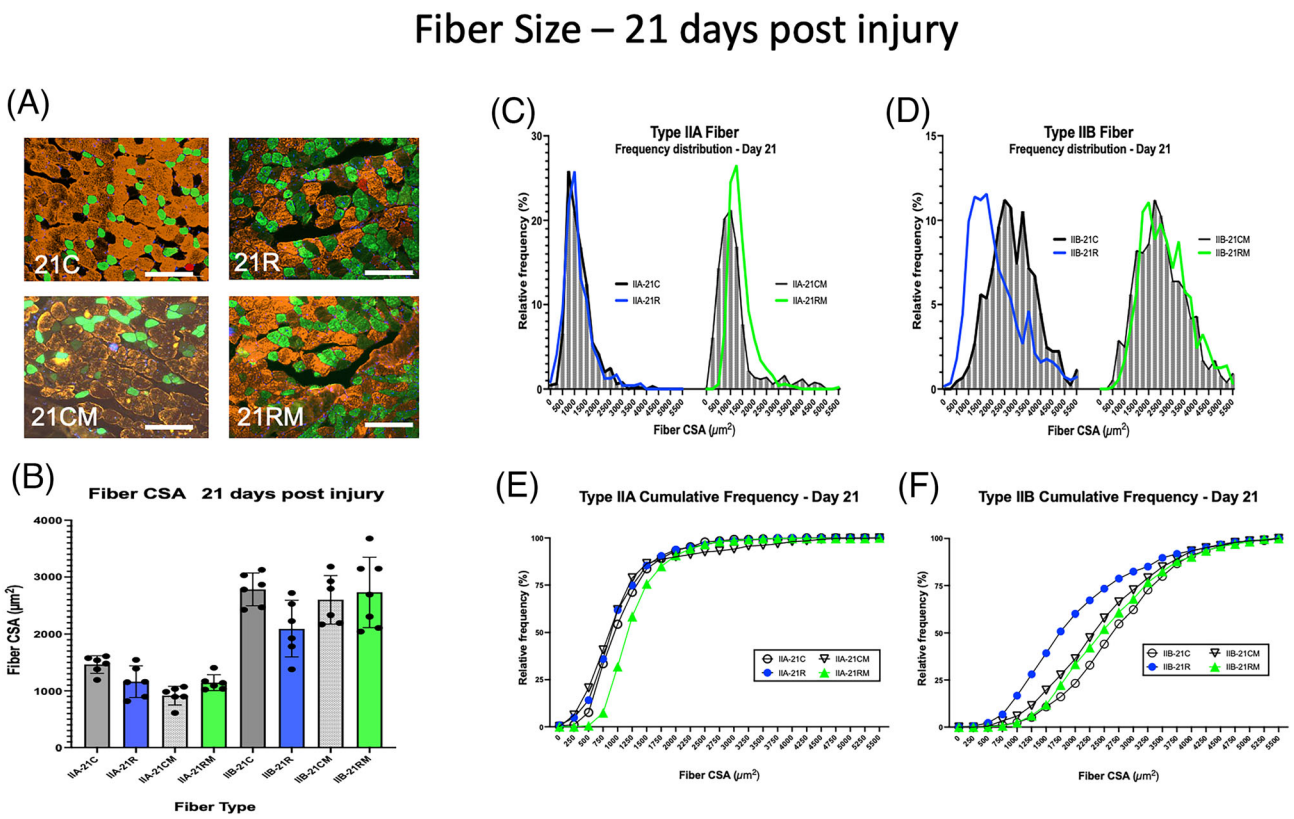

Figure 6 Muscle fibre size 21 days after $BaCl_2$ injury. (*A*) Examples of gastrocnemius cross sections of uninjured control muscles of phosphate-buffered saline (PBS)-treated mice (21C) or mitochondrial transplant therapy (MTT)-treated mice (21CM). Examples of muscle cross sections are shown where injured muscles were allowed to repair for 21 days after systemic PBS treatment (21R) and systemic MTT treatment (21RM). Fibre type was identified by immunocytochemistry of myosin heavy chains. Type IIA fibres (green), Type IIB fibres (orange/gold), Type IIX fibres (black) and Type I fibres (red). The white bar is 200 μm in length. (*B*) Examples of gastrocnemius cross sections of uninjured control muscles of phosphate-buffered saline (PBS)-treated mice (21C) or mitochondrial transplant therapy (MTT)-treated mice (21CM). Examples of muscle cross sections are shown where injured muscles were allowed to repair for 21 days after systemic PBS treatment (21R) and systemic MTT treatment (21RM). Fibre type was identified by immunocytochemistry of myosin heavy chains. Type IIA fibres (green), Type IIB fibres (orange/gold), Type IIX fibres (black) and Type I fibres (red). The white bar is 200 μm in length. (*SD* for each animal. Control non-injured (PBS injected) muscles from PBS sham-treated (21C) or MTT-treated mice (21CM). Injured ($BaCl_2$ injected) muscles from PBS-treated (21R) or MTT-treated mice (21RM). (*C–F*) Fibre frequency histograms (*C,D*) and cumulative frequency distributions (*E,F*) for Type IIA (*C,E*) and Type IIB (*D,F*) fibres. (*C,D*) The corresponding control non-injured muscle data for the frequency histograms (21C or 21CM) are represented by shaded bars. The blue line represents data from PBS sham-treated mice 14 days post-injury (21R). The green line represents data from MTT-treated mice after 14 days of injury (21RM). (*E,F*) Cumulative frequency distribution for non-damaged control muscle data (21C, circle or 21CM, inverted triangle). The blue line, PBS-injected mice 21 days post-injury (21R). The green line, MTT-injected mice after 21 days of injury (21RM).

was similar in the gastrocnemius of 7R and 7RM mice. Similarly, maximal muscle force was reduced to a similar level in 7R and 7RM muscles after BaCl2 injury (*Figure 3B*). MTT did not appear to improve the overall repair of Type IIA or Type IIB fibres by 7 days post-injury, because mean fibre CSA, mean Feret diameter and the cumulative frequency distribution of Types IIA and IIB fibres were similar in 7R and 7RM muscles (*Figures 4B* and *S5A–C*). Together, these data show that the extent of the initial 7 days of muscle regeneration after injury was not improved by MTT. While the early events of MSC proliferation and differentiation are critical to the initiation of muscle repair,[40,41] MSC activation was not evaluated in this study. The failure to improve the early stages of muscle repair was not the result of the donor mitochondria initiating an inflammatory state in MTT-treated mice, because the systemic delivery of mitochondria did not elevate CRP or IFN-γ, which are markers for systemic inflammation (*Figure 7F,G*).

PBS-treated mice had no improvement in plantar flexor muscle force, muscle wet weight or mean Type IIB fibre size between 7 and 14 days of repair following injury, as compared with the uninjured control muscles. In contrast, maximal muscle force showed significant recovery in MTT-treated mice 14 days after injury compared with the maximal plantar flexor force levels achieved 7 days after injury, or in comparison to maximal force production of undamaged control muscles of MTT-treated animals (*Figure 3B*). This greater restoration of muscle force by

DOI: 10.1002/jcsm.13153

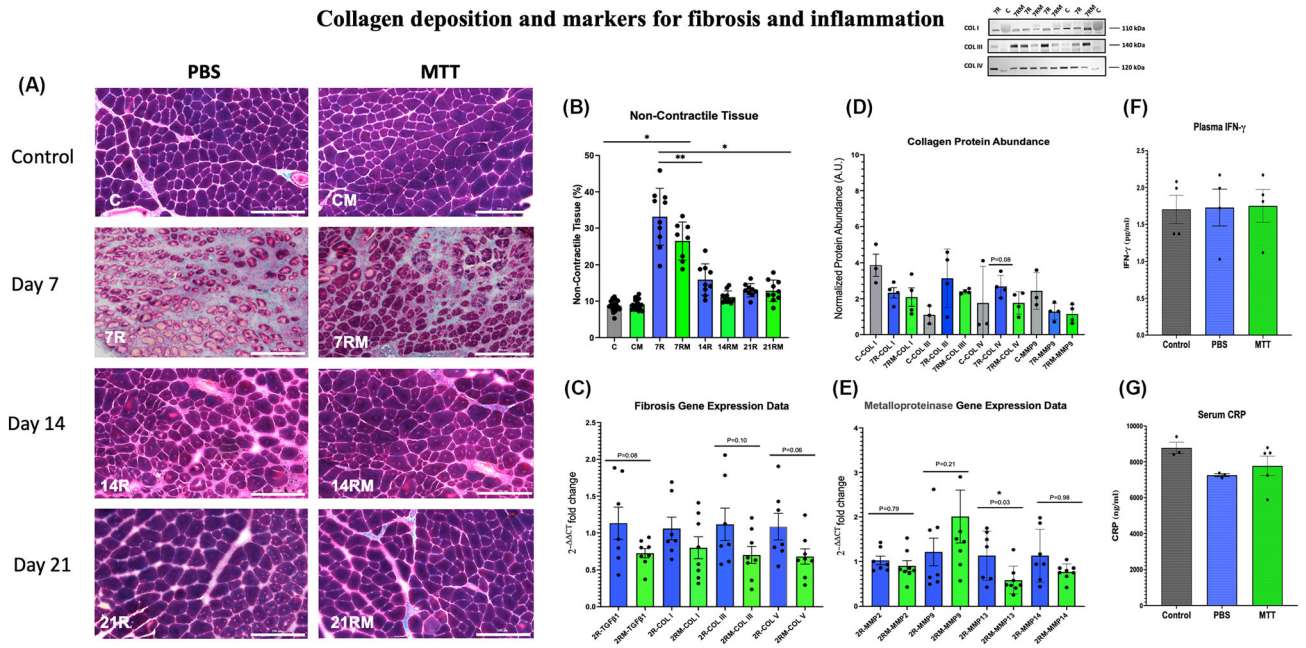

Figure 7 Collagen deposition and markers for fibrosis and for inflammation. (*A*) *Gomori's trichrome non-contractile collagen staining*. Examples of tissue cross sections of control and injured gastrocnemius muscles after phosphate-buffered saline (PBS) or mitochondrial transplant therapy (MTT) treatment. Collagen fibres were identified with Gomori's trichrome staining in gastrocnemius tissue cross sections from PBS-treated or MTT-treated mice after 7 days (7R,7RM), 14 days (14R, 14RM) or 21 days (21R, 21RM) of injury. The white bar is 200 μm in length. (*B*) *Quantification of the non-contractile and collagen tissue*. Collagen deposition was quantified stereologically by a 224-point count grid and the percentage of the total fibre tissue section was presented as mean ± *SD*. Control non-injured PBS sham-treated muscles (*C*), and MTT-treated muscles (CM). PBS repairing muscles 7 (7R), 14 (14R) and 21 days (21R) after injury and mitochondria-treated repairing muscles after 7 (7RM), 14 (14RM), 21 (21RM) days after injury. $*P < 0.05$, versus 7R and 7 RM; $**P < 0.05$, Day 7R versus Day 7RM. (*C*) *Collagen/fibrosis gene markers.* Gastrocnemius muscles were injured by $BaCl_2$ and injected with PBS or MTT 24 h after the muscle injury. mRNA was isolated from muscles 48 h after the initial injury. The relative expression levels of amplified transcripts were estimated by the comparative CT method ($2^{-\Delta\Delta CT}$) and normalized to a house keeping gene (*GAPDH*). The temperature cycle profile for the qPCR reactions was 50°C for 2 min 95°C for 10 s followed by 40 cycles of 95°C for 15 s and 60°C for 60 s. A melt curve of 95°C for 15 s, 60°C for 60 s, and 95°C for 15 s was used to verify the specificity of the amplified PCR product. The data were expressed as fold-differences compared with the uninjured intra-animal control muscle. mRNA expression was measured by qPCR for genes that are indicators of fibrosis and collagen signalling (*TGFβ1*). The temperature cycle profile for the qPCR reactions was 50°C for 2 min 95°C for 10 s followed by 40 cycles of 95°C for 15 s and 60°C for 60 s. A melt curve of 95°C for 15 s, 60°C for 60 s, and 95°C for 15 s was used to verify the specificity of the amplified PCR product. The data were expressed as fold-differences compared with the uninjured intra-animal control muscle. mRNA expression was measured by qPCR for genes that are indicators of fibrosis and collagen signalling (*COL I*, *COL III* and *COL V*). The data are expressed as the fold change of $2^{-\Delta\Delta CT}$ from injured as compared with control muscles. (*D*) *Collagen protein abundance.* The gastrocnemius muscle of one limb was injured by $BaCl_2$, and the contralateral limb was injected with PBS which did not cause muscle injury. Twenty-four hours after the injury, mice received a systemic injection of PBS or MTT. Approximately 40 mg of muscle was homogenized, and cell lysates were separated on SDS-polyacrylamide gels then transferred to polyvinylidene fluoride (PVDF) membranes. The membranes were blocked in 5% bovine serum albumin (BSA) and total protein was fluorescently quantified via the iBright FL1500 imaging system (Invitrogen). The membranes were then incubated overnight at 4°C with primary antibodies for Collagen I (alpha 2(I) chain with a predicted molecular weight ~110 kDa), Collagen III (molecular weight ~140 kDa) or Collagen IV (molecular weight ~120 kDa). The membranes were washed and incubated with anti-rabbit or anti-mouse IgG-conjugated secondary antibodies then the signals were developed with SuperSignal West Pico plus ECL reagent and imaged. The proteins were then quantified by ImageJ. The data show that MTT had a tendency ($P = 0.08$) to suppress Collagen IV protein abundance in injured-repairing muscles, 7 days after injury. An example of western blots for Collagen I (COL I), Collagen III (COL 3) and Collagen IV (COL IV) are shown in the insert. (*C*) Control uninjured muscles; 7R, PBS-treated muscles, 7 days after injury; 7RM, MTT-treated muscles, 7 days after injury. (*E*) *Metalloproteinase mRNA*. Transcript levels were determined for metal metalloproteinases (MMP2, MMP9, MMP13 and MMP14) to determine if MTT affected collagen/fibrosis remodelling during muscle repair after an injury. The gastrocnemius muscle of one limb was injured by $BaCl_2$ injection, while the opposite limb received PBS as a non-injury control. Twenty-four hours after injury, mice received a systemic injection of PBS or MTT. The muscles were harvested, and mRNA was isolated from muscles 48 h after the initial injury. The relative expression levels of amplified transcripts were estimated by the comparative CT method ($2^{-\Delta\Delta CT}$) and normalized to a house keeping gene (*GAPDH*). The temperature cycle profile for the qPCR reactions was 50°C for 2 min 95°C for 10 s followed by 40 cycles of 95°C for 15 s and 60°C for 60 s. a melt curve of 95°C for 15 s, 60°C for 60 s, and 95°C for 15 s was used to verify the specificity of the amplified PCR product. The data were expressed as fold differences compared with the uninjured intra-animal control muscle. This suggests that signalling for fibrosis/non-contractile tissue tended to have lower mRNA in injured muscles from MTT- than PBS-treated animals 2 days of injury. $*P < 0.05$, versus 2R MMP13 versus 2RM MMP13. All other data failed to reach significance. The *P* values shown on the figure. (*F*) *Plasma levels of IFN-γ*. Plasma levels of IFN-γ were measured by ELISA in control naive non-injured mice ($n = 4$), and 48 h after systemic injection of either PBS ($n = 4$) or MTT ($n = 4$). Data are presented as mean ± *SD*. Mice did not receive a muscle injury in these exper-

DOI: 10.1002/jcsm.13153

iments, to identify whether MTT created a systemic inflammatory response in the mice. No increases in IFN-γ were identified by systemic delivery of MTT. (*G*) *C-reactive protein* (*CRP*). Plasma levels of CRP were measured as a second marker of systemic inflammation. CRP was detected by an ELISA in control naive non-injured, non-treated mice (n = 3), and 48 h after systemic injection into the tail vein mice for PBS (n = 3) or MTT (n = 4). No increase in CRP was identified after systemic delivery of mitochondria to the mice 2 days after systemic injection, as compared with PBS-treated or non-treated animals.

MTT was due at least in part to greater regeneration of contractile tissue. Both gastrocnemius muscle weight (*Figure 3C*) and Type IIB fibre size (*Figure 5B,C*) were greater in 14RM versus 14R muscles, or as compared with injured muscles of either 7R or 7RM mice. The MTT improvement in regeneration appeared to be fibre-type specific because mean fibre area, fibre area frequency and cumulative fibre area were all similar in repairing Type IIA fibres of MTT-treated and PBS-treated mice 14 days after injury. Thus, the improved repair of both force and muscle structure in the gastrocnemius of MTT-treated mice appeared to be limited to Type IIB fibres. Enhanced Type IIB repair is important because this is the primary fibre type of the mouse gastrocnemius.

The slower restoration of Type IIB fibre size in PBS as compared with MTT-treated mice as shown by a lower maximal force production, as well as the differences in the cumulative frequency and fibre area distributions at 14 and 21 days following injury, suggests that mitochondrial supplementation is most effective during the periods of anabolic growth and signalling in differentiated muscle cells. We do not know if this response is unique to the gastrocnemius; however, we speculate that because Type IIB fibres generally contain a low percentage of mitochondria, they may benefit more from MTT in muscle repair as compared with fibres having a higher percentage of mitochondria such as Type IIA or Type I fibres.[42] It is possible that Type IIA fibres had sufficient mitochondria for fibre repair so that additional mitochondria were not advantageous for their repair. Alternatively, uninjured Type IIA fibres may have donated healthy mitochondria to the injury site and improved repair without the need to supplement repair with more mitochondria. Nevertheless, it is worth noting that this may not be the reason for this observation because MTT has been shown to improve myocardial repair after ischaemia–reperfusion injury[35,43,44] and myocardial cells contain a high volume of mitochondria.

Although wet weight and fibre CSA were restored to control levels in the PBS-treated muscles 21 days post-injury, Type IIB fibre area-frequency and cumulative frequency distributions indicated that all Type IIB fibres had not been fully restored. In contrast, Type IIB fibre area and gastrocnemius muscle force were fully restored to control levels by 21 days after injury in MTT-treated mice compared with non-injured contralateral control muscles. Together, these findings suggest that MTT had accelerated the restoration of neuromuscular force and Type IIB fibre size compared with PBS-treated muscles after $BaCl_2$ injury.

Mitochondrial transplant therapy regulation of non-contractile tissue

Stereological analysis from tissue cross sections showed significantly greater collagen in $BaCl_2$-damaged muscles of PBS-treated mice compared with MTT-treated mice 7 days after injury. However, non-contractile/collagen tissue in cross sections began to decline (i.e., remodel) by 14 days after injury, in both PBS sham- and MTT-treated muscles. The initial remodelling of collagen and other non-contractile tissue elements could have been influenced by differences in inflammation between PBS- and MTT-treated mice, as suggested by a tendency for a decline in mRNA for TGFβ, Collagen III and IV mRNA in muscles from MTT-treated mice. Furthermore, we found a tendency for lower collagen transcripts and Collagen IV protein abundance in MTT-treated muscles after injury, but additional work is needed to establish the importance of MTT regulation of collagen/fibrosis as an early response mechanism in muscle repair. We also found that the transcript level of MMP13, a major enzyme that targets connective tissue for degradation,[45] was significantly lower in injured muscles from MTT compared with PBS-treated mice 48 h after injury, and this is consistent with an MTT regulation of collagen deposition, although neither the protein abundance nor transcripts for MMP9 appeared to be altered in repairing muscle from PBS as compared with MTT-treated mice.

This study was not designed to address the mechanism by which MTT might improve muscle repair. Nevertheless, our data show a therapeutic role for MTT and that donor mitochondria are taken up by muscle cells in vitro. Furthermore, injured muscle cells in vivo appear to preferentially incorporate donor mitochondria as compared with non-injured muscle fibres. One possibility is that the damaged muscle membranes eliminated a barrier for mitochondria, which allowed damaged fibres to accumulate donor mitochondria after MTT. However, if this is the case, we do not know if this is a passive accumulation through damaged membranes or if there is a specific signal that attracts the donor mitochondria to the injury site. Furthermore, it is possible that their overall purpose may at least in part be in regulating molecular signalling during muscle repair. Although speculative, we hypothesize that the importance of donor mitochondria may go beyond simply providing additional ATP to the repairing muscle. This is hinted in the tendency for an MTT-induced reduction of collagen mRNA and collagen protein abundance in the extracellular matrix of repairing muscle, although the importance of this is not yet clear.

Limitations

This study had several limitations. Although MTT showed improved force recovery, and Type IIB fibre size after $BaCl_2$ injury, further investigation is needed to determine if a single treatment of MTT provides a maximal repair response or if multiple applications of MTT will further improve muscle repair and/or accelerate the restoration of neuromuscular junction remodelling and the ability to generate muscle force. Furthermore, we do not know if MTT will provide similar benefits during repair from an injury that was not induced by $BaCl_2$. Finally, we do not know if mitochondrial signalling or additional mitochondrial oxidative phosphorylations are most important during MTT-enhanced muscle repair or how long donor mitochondria persist after transplantation for contributing to muscle repair.

Conclusions

This study showed that MTT one day after injury did not induce a systemic inflammation nor did it modulate the functional repair of muscle over the first week following injury. However, MTT had a tendency for lower non-contractile collagen deposition and significantly improved the rate of gastrocnemius muscle fibre repair and restoration of force, especially between 7 and 14 days following $BaCl_2$ injury. Thus, MTT enhanced regeneration preferentially in Type IIB fibres and improved restoration of muscle function following injury.

Acknowledgements

This project has been funded by W81XWH2110187 from the U.S. Army Medical Research and Development Command, U.S. Department of Defense awarded to SEA. The antibodies BA-F8, SC-71 and BF-F3 were developed by Dr. S. Schiaffino, and the antibody and MandyS8(8H11) was developed by G. E. Morris. These antibodies were obtained from the Developmental Studies Hybridoma Bank developed under the auspices of the NICHD and maintained by the University of Iowa, Department of Biology, Iowa City, IA 52242, USA. The authors certify that they comply with the ethical guidelines for authorship and publishing of the *Journal of Cachexia, Sarcopenia and Muscle*.[46]

Conflict of interest

Stephen E. Alway, Hector G. Paez, Christopher R. Pitzer, Peter J. Ferrandi, Mohammad Moshahid Khan, Junaith S. Mohamed, James A. Carson and Michael R. Deschenes declare that they have no conflict of interest.

Online supplementary material

Additional supporting information may be found online in the Supporting Information section at the end of the article.

References

1. Hood DA, Memme JM, Oliveira AN, Triolo M. Maintenance of skeletal muscle mitochondria in health, exercise, and aging. *Annu Rev Physiol* 2019;**81**:19–41.
2. Alway SE, Mohamed JS, Myers MJ. Mitochondria initiate and regulate sarcopenia. *Exerc Sport Sci Rev* 2017;**45**:58–69.
3. Favaro G, Romanello V, Varanita T, Andrea Desbats M, Morbidoni V, Tezze C, et al. DRP1-mediated mitochondrial shape controls calcium homeostasis and muscle mass. *Nat Commun* 2019;**10**:2576.
4. Vezzoli M, Castellani P, Corna G, Castiglioni A, Bosurgi L, Monno A, et al. High-mobility group box 1 release and redox regulation accompany regeneration and remodeling of skeletal muscle. *Antioxid Redox Signal* 2011;**15**:2161–2174.
5. Bellot GL, Dong X, Lahiri A, Sebastin SJ, Batinic-Haberle I, Pervaiz S, et al. MnSOD is implicated in accelerated wound healing upon Negative Pressure Wound Therapy (NPWT): a case in point for MnSOD mimetics as adjuvants for wound management. *Redox Biol* 2019;**20**:307–320.
6. Del Campo A, Contreras-Hernandez I, Castro-Sepulveda M, Campos CA, Figueroa R, Tevy MF, et al. Muscle function decline and mitochondria changes in middle age precede sarcopenia in mice. *Aging (Albany NY).* 2018;**10**:34–55.
7. Moreira OC, Estebanez B, Martinez-Florez S, de Paz JA, Cuevas MJ, Gonzalez-Gallego J. Mitochondrial function and mitophagy in the elderly: effects of exercise. *Oxid Med Cell Longev* 2017;**2017**:2012798.
8. Porter C, Hurren NM, Cotter MV, Bhattarai N, Reidy PT, Dillon EL, et al. Mitochondrial respiratory capacity and coupling control decline with age in human skeletal muscle. *Am J Physiol Endocrinol Metab* 2015;**309**:E224–E232.
9. Yan Z, Lira VA, Greene NP. Exercise training-induced regulation of mitochondrial quality. *Exerc Sport Sci Rev* 2012;**40**:159–164.
10. Rigoulet M, Yoboue ED, Devin A. Mitochondrial ROS generation and its regulation: mechanisms involved in H_2O_2 signaling. *Antioxid Redox Signal* 2011;**14**:459–468.
11. Brooks MJ, Hajira A, Mohamed JS, Alway SE. Voluntary wheel running increases satellite cell abundance and improves recovery from disuse in gastrocnemius muscles from mice. *J Appl Physiol* 1985;**2018**:1616–1628.
12. Hwang AB, Brack AS. Muscle Stem Cells and Aging. *Curr Top Dev Biol* 2018;**126**:299–322.
13. Mathew SJ, Hansen JM, Merrell AJ, Murphy MM, Lawson JA, Hutcheson DA, et al. Connective tissue fibroblasts and Tcf4 regulate myogenesis. *Development* 2011;**138**:371–384.
14. Murphy MM, Lawson JA, Mathew SJ, Hutcheson DA, Kardon G. Satellite cells, connective tissue fibroblasts and their interactions are crucial for muscle regeneration. *Development* 2011;**138**:3625–3637.
15. Purushotham A, Schug TT, Xu Q, Surapureddi S, Guo X, Li X. Hepatocyte-specific deletion of SIRT1 alters fatty acid metabolism and results in hepatic steatosis

and inflammation. *Cell Metab* 2009;**9**: 327–338.
16. Myers MJ, Shepherd DL, Durr AJ, Stanton DS, Mohamed JS, Hollander JM, et al. The role of SIRT1 in skeletal muscle function and repair of older mice. *J Cachexia Sarcopenia Muscle* 2019;**10**:929–949.
17. Dulac M, Leduc-Gaudet JP, Cefis M, Ayoub MB, Reynaud O, Shams A, et al. Regulation of muscle and mitochondrial health by the mitochondrial fission protein Drp1 in aged mice. *J Physiol* 2021;**599**:4045–4063.
18. Dulac M, Leduc-Gaudet JP, Reynaud O, Ayoub MB, Guerin A, Finkelchtein M, et al. Drp1 knockdown induces severe muscle atrophy and remodelling, mitochondrial dysfunction, autophagy impairment and denervation. *J Physiol* 2020;**598**: 3691–3710.
19. Maezawa T, Tanaka M, Kanazashi M, Maeshige N, Kondo H, Ishihara A, et al. Astaxanthin supplementation attenuates immobilization-induced skeletal muscle fibrosis via suppression of oxidative stress. *J Physiol Sci* 2017;**67**:603–611.
20. McCully JD, Levitsky S, Del Nido PJ, Cowan DB. Mitochondrial transplantation for therapeutic use. *Clin Transl Med* 2016;**5**:16.
21. Kaza AK, Wamala I, Friehs I, Kuebler JD, Rathod RH, Berra I, et al. Myocardial rescue with autologous mitochondrial transplantation in a porcine model of ischemia/reperfusion. *J Thorac Cardiovasc Surg* 2017;**153**:934–943.
22. Preble JM, Pacak CA, Kondo H, MacKay AA, Cowan DB, McCully JD. Rapid isolation and purification of mitochondria for transplantation by tissue dissociation and differential filtration. *J Vis Exp* 2014;e51682.
23. Ali Pour P, Kenney MC, Kheradvar A. Bioenergetics consequences of mitochondrial transplantation in cardiomyocytes. *J Am Heart Assoc* 2020;**9**:e014501.
24. Orfany A, Arriola CG, Doulamis IP, Guariento A, Ramirez-Barbieri G, Moskowitzova K, et al. Mitochondrial transplantation ameliorates acute limb ischemia. *J Vasc Surg* 2019;1014–1026.
25. Paliwal S, Chaudhuri R, Agrawal A, Mohanty S. Regenerative abilities of mesenchymal stem cells through mitochondrial transfer. *J Biomed Sci* 2018;**25**:31.
26. Sasaki D, Abe J, Takeda A, Harashima H, Yamada Y. Transplantation of MITO cells, mitochondria activated cardiac progenitor cells, to the ischemic myocardium of mouse enhances the therapeutic effect. *Sci Rep* 2022;**12**:4344.
27. George RM, Biressi S, Beres BJ, Rogers E, Mulia AK, Allen RE, et al. Numb-deficient satellite cells have regeneration and proliferation defects. *Proc Natl Acad Sci U S A* 2013;**110**:18549–18554.
28. Komlodi T, Sobotka O, Krumschnabel G, Bezuidenhout N, Hiller E, Doerrier C, et al. Comparison of mitochondrial incubation media for measurement of respiration and hydrogen peroxide production. *Methods Mol Biol* 2018;**1782**:137–155.
29. Gnaiger E. Mitochondrial pathways and respiratory control: an introduction to OXPHOS analysis. *Bioenerget Commun* 2020A;**2020**:122.
30. Aragones J, Schneider M, Van Geyte K, Fraisl P, Dresselaers T, Mazzone M, et al. Deficiency or inhibition of oxygen sensor Phd1 induces hypoxia tolerance by reprogramming basal metabolism. *Nat Genet* 2008;**40**:170–180.
31. Mohamed JS, Wilson JC, Myers MJ, Sisson KJ, Alway SE. Dysregulation of SIRT-1 in aging mice increases skeletal muscle fatigue by a PARP-1-dependent mechanism. *Aging (Albany NY)* 2014;**10**:820–834.
32. Myers MJ, Shaik F, Shaik F, Alway SE, Mohamed JS. Skeletal muscle gene expression profile in response to caloric restriction and aging: a role for SirT1. *Genes (Basel)* 2021;**12**:691.
33. Alway SE, Winchester PK, Davis ME, Gonyea WJ. Regionalized adaptations and muscle fiber proliferation in stretch-induced enlargement. *J Appl Physiol* 1985;**1989**:771–781.
34. Emani SM, Piekarski BL, Harrild D, Del Nido PJ, McCully JD. Autologous mitochondrial transplantation for dysfunction after ischemia-reperfusion injury. *J Thorac Cardiovasc Surg* 2017;**154**:286–289.
35. Shin B, Cowan DB, Emani SM, Del Nido PJ, McCully JD. Mitochondrial Transplantation in Myocardial Ischemia and Reperfusion Injury. *Adv Exp Med Biol* 2017;**982**: 595–619.
36. McCully JD, Cowan DB, Emani SM, Del Nido PJ. Mitochondrial transplantation: From animal models to clinical use in humans. *Mitochondrion* 2017;**34**:127–134.
37. Morton AB, Norton CE, Jacobsen NL, Fernando CA, Cornelison DDW, Segal SS. Barium chloride injures myofibers through calcium-induced proteolysis with fragmentation of motor nerves and microvessels. *Skelet Muscle* 2019;**9**:27.
38. Khan MM, Paez HG, Pitzer CR, Alway SE. The therapeutic potential of mitochondria transplantation therapy in neurodegenerative and neurovascular disorders. *Curr Neuropharmacol* 2022;**20**.
39. Ali Pour P, Hosseinian S, Kheradvar A. Mitochondrial transplantation in cardiomyocytes: foundation, methods, and outcomes. *Am J Physiol Cell Physiol* 2021;**321**: C489–C503.
40. Brack AS, Rando TA. Tissue-specific stem cells: lessons from the skeletal muscle satellite cell. *Cell Stem Cell* 2012;**10**:504–514.
41. Feige P, Brun CE, Ritso M, Rudnicki MA. Orienting muscle stem cells for regeneration in homeostasis, aging, and disease. *Cell Stem Cell* 2018;**23**:653–664.
42. Bloemberg D, Quadrilatero J. Rapid determination of myosin heavy chain expression in rat, mouse, and human skeletal muscle using multicolor immunofluorescence analysis. *PLoS One* 2012;**7**:e35273.
43. Emani SM, McCully JD. Mitochondrial transplantation: applications for pediatric patients with congenital heart disease. *Transl Pediatr* 2018;**7**:169–175.
44. Blitzer D, Guariento A, Doulamis IP, Shin B, Moskowitzova K, Barbieri GR, et al. Delayed transplantation of autologous mitochondria for cardioprotection in a porcine model. *Ann Thorac Surg* 2020;**109**:711–719.
45. Vincenti MP, Brinckerhoff CE. Transcriptional regulation of collagenase (MMP-1, MMP-13) genes in arthritis: integration of complex signaling pathways for the recruitment of gene-specific transcription factors. *Arthritis Res* 2002;**4**:157–164.
46. von Haehling S, Morley JE, Coats AJS, Anker SD. Ethical guidelines for publishing in the *Journal of Cachexia, Sarcopenia and Muscle*: update 2021. *J Cachexia Sarcopenia Muscle* 2021;**12**:2259–2261.